

Optimal Disturbances in Swirling Flows

Guy Ben-Dov,* Vladimir Levinski,[†] and Jacob Cohen[‡]
Technion—Israel Institute of Technology, 32000 Haifa, Israel

The mechanism of optimal disturbances, which are composed of both growing and decaying modes, in swirling flows (with an axial velocity component) is explored. Two characterizing cases are considered: stationary disturbances in rotating pipe flow and temporal disturbances in a trailing vortex. It is found that in both cases the optimal transient growth amplification in short times or distances is much larger than the known exponential mode amplification. Unlike the flow in a nonrotating pipe, in which the amplification is based on the existence of a least stable pair of modes and the cancellation of their associated initial axial velocity components, when a rotation is added to the flow the optimal amplification mechanism is based on the cancellation, at the initial state, of the most unstable mode velocity components by many decaying modes. For the trailing vortex, the transient growth mechanism seems to be based on the contribution of the continuous spectrum, and the optimal transient growth is not significantly affected by the existence of swirl in the flow. Evidently, when the flow is unstable with respect to discrete exponential modes, decaying modes still may have a substantial contribution for the linear stability of the flow in short times or distances, assuming the existence of a particular initial disturbance.

Introduction

FOR many years transition to turbulence has been studied by considering only periodic disturbances that are modal in nature. The study of algebraic growth of nonmodal disturbances in shear flows has become of great interest during the past decade because it was shown to be associated with bypass transition.

The significant algebraic growth, which can be achieved by the nonmodal disturbances, raises the possibility that the transition of certain types of shear flows that are linearly unstable due to an exponential growth mechanism of a single mode may be actually dominated by a multiple-mode mechanism. In this study, we investigate the possible growth of optimal nonmodal disturbances in swirling flows (with an axial velocity component), as an example for such type of flow.

The linear stability of swirling flows has been investigated since the 1880s, when both Rayleigh and Kelvin studied various aspects of the simplified inviscid stability problem. Since then, and in particular after the discovery of vortex breakdown phenomena on slender wings at high angles of attack during wind-tunnel tests in the late 1950s, it has become a primary subject of research.

Many studies have been carried out in the field of hydrodynamic stability of swirling flows, assuming small disturbances and columnar base flow. Most of this work was summarized in the detailed review paper by Ash and Khorrami.¹ A major part of these classical reports were concerned with the temporal evolution of discrete modes, including several stability criteria and circle theorems by Howard and Gupta,² Leibovich and Stewartson,³ and Barston.⁴ In many studies, the temporal stability of a trailing vortex (Batchelor vortex) was investigated, including reports by Lessen et al.⁵ and Mayer and Powell⁶ for inviscid flow and reports by Lessen and Paillet,⁷ Khorrami,⁸ and Mayer and Powell⁶ for viscous flow. In

these studies, discrete growing modes were found for various swirl parameters in the inviscid case and for various combinations of swirls and Reynolds numbers in the viscous case.

More recently, the absolute-convective inviscid instability of columnar swirling flows was studied to map the unstable discrete modes for various swirl parameters and to find critical points where the flow becomes absolutely unstable. Delbende et al.⁹ and Olen-drar et al.¹⁰ carried out an absolute-convective analysis for the trailing vortex, and Loiseleux et al.¹¹ analyzed the Rankine vortex with uniform axial flow.

To the best of our knowledge, all of the studies concerning the linear stability of swirling flows with an axial velocity component analyze discrete modes that exponentially grow in time and/or in space. In this paper, we show that, when an initial disturbance is assumed, a significant transient growth may be obtained in short times (or distances). In fact, an optimal initial disturbance that yields the maximum amplification of the disturbance energy density in short times (or distances) can be found. Its energy growing rate is orders of magnitude larger than the corresponding growing rate of the most unstable discrete mode. In short times (or distances), such optimal initial disturbances may trigger nonlinear mechanisms and bypass the discrete mode exponential growth.

One of the first known reports demonstrating this kind of algebraic growth is that by Elingsen and Palm,¹² who considered a three-dimensional inviscid linear disturbance for which the velocity was assumed to be uniform in the flow direction. Benney and Gustavsson¹³ suggested that a three-dimensional viscous small disturbance may produce a direct resonance, giving rise to a linear growth in short times. The concept of direct resonance between decaying modes lead to the investigation of a possible transient growth due to the interaction between similar decaying modes of a viscous disturbance. Henningson¹⁴ suggested that a significant transient growth is achieved by the interference of many decaying modes, when these modes are nonorthogonal and their eigenfunctions are very close to be parallel. As the Reynolds number of the flow is increased, the more parallel the eigenfunctions tend to be, causing the amplification of the initial disturbance to be larger. A vast bibliography on transient growth can be found in the Otto Laporte Award Lecture by Reshotko¹⁵ and in the monograph by Schmid and Henningson.¹⁶

Henningson¹⁴ and later Henningson et al.¹⁷ presented results for a significant transient growth in channel flows, where a specific initial condition was chosen. They found that a typical initial condition that yields the most significant transient growth is the one having only vertical velocity component and no vorticity. Similarly, for circular pipe flow O'Sullivan and Breuer¹⁸ chose the initial disturbance to have only radial velocity and no radial vorticity. The evolution of

Presented as Paper 2003-3594 at the AIAA 33rd Fluid Dynamics Conference, Orlando, FL, 23–26 June 2003; received 16 October 2003; revision received 25 March 2004; accepted for publication 19 April 2004. Copyright © 2004 by the authors. Published by the American Institute of Aeronautics and Astronautics, Inc., with permission. Copies of this paper may be made for personal or internal use, on condition that the copier pay the \$10.00 per-copy fee to the Copyright Clearance Center, Inc., 222 Rosewood Drive, Danvers, MA 01923; include the code 0001-1452/04 \$10.00 in correspondence with the CCC.

*Graduate Student, Faculty of Aerospace Engineering; guyb@aerodyne.technion.ac.il.

[†]Senior Research Associate, Faculty of Aerospace Engineering; currently Senior Algorithm Design Engineer, Optical Metrology, KLA-Tencor Corporation, 23100 Migdal Ha'Emek, Israel; vladimir.levinsky@kla-tencor.com.

[‡]Associate Professor, Faculty of Aerospace Engineering; aerycyc@aerodyne.technion.ac.il. Member AIAA.

a three-dimensional disturbance can produce a significant vertical vorticity, where the nonhomogeneous part of the vertical vorticity equation yields a lift-up effect.

The transient growth mechanism strongly depends on the form of the initial condition, and this fact naturally raises thoughts about the possibility of optimizing the initial condition to give maximum transient growth amplification. Gustavsson¹⁹ presented results for transient growth in plane Poiseuille flow and suggested the disturbance kinetic energy density as a physical functional that is appropriate as a measure for the transient growth amplification. Butler and Farrell²⁰ used a variational technique to calculate such optimal disturbances. Reddy and Henningson²¹ studied various aspects of the transient growth of the disturbance energy density in channel flows, using energy methods and a direct numerical procedure. Bergström²² considered optimal disturbances analysis in pipe Poiseuille flow using the variational technique, whereas Schmid and Henningson²³ used the direct numerical procedure proposed by Reddy and Henningson²¹ for optimizing the initial disturbances in the same type of flow. Reshotko and Tumin²⁴ used this numerical scheme to investigate optimal growth of spatial disturbances in pipe flows. Unlike the temporal case, they had to exclude the upstream eigenmodes in their analysis, following from the consideration of the signaling problem (e.g., see Ashpis and Reshotko²⁵). Ben-Dov et al.²⁶ showed that the most amplified optimal disturbances, in this case of nonrotating pipe flow, are dominated by a pair of nearly parallel least stable modes (having opposite phases and almost identical amplitude distributions). Accordingly, the time and distance, at which the maximum energy amplification of an initial disturbance is achieved, are well predicted analytically by considering only the pair of least stable modes. Furthermore, the dependence of the maximum energy amplification on the Reynolds number matches previous numerical results based on the analysis of many modes.

The purpose of the present work is to show that although exponential modes exist in swirling shear flows, the transient growth of certain disturbances may be orders of magnitude larger. The paper begins with a short mathematical background of the initial value problem and the optimal disturbances formulation in cylindrical flows. Then results for two representative cases are presented: The first case is concerned with spatial disturbances in a rotating pipe flow, whereas the second case deals with temporal disturbances in a trailing vortex.

Mathematical Background

Initial Value Problem

Our starting point for the analysis of small disturbances in cylindrical flow is the linearized Navier–Stokes equations for incompressible flow in cylindrical coordinates. A columnar mean flow of the form $\{U, V, W\} = \{0, V(r), W(r)\}$ is assumed, where U , V , and W are the mean flow radial, azimuthal, and axial velocity components, respectively. The governing equations in this case are

$$\frac{\partial u}{\partial t} + \frac{V}{r} \frac{\partial u}{\partial \theta} + W \frac{\partial u}{\partial z} - 2 \frac{Vv}{r} = -\frac{\partial p}{\partial r} + \frac{1}{Re} \left(\nabla^2 u - \frac{u}{r^2} - \frac{2}{r^2} \frac{\partial v}{\partial \theta} \right) \quad (1)$$

$$\begin{aligned} \frac{\partial v}{\partial t} + u \frac{\partial V}{\partial r} + \frac{V}{r} \frac{\partial v}{\partial \theta} + W \frac{\partial v}{\partial z} + \frac{Vu}{r} \\ = -\frac{1}{r} \frac{\partial p}{\partial \theta} + \frac{1}{Re} \left(\nabla^2 v - \frac{v}{r^2} + \frac{2}{r^2} \frac{\partial u}{\partial \theta} \right) \end{aligned} \quad (2)$$

$$\frac{\partial w}{\partial t} + u \frac{\partial W}{\partial r} + \frac{V}{r} \frac{\partial w}{\partial \theta} + W \frac{\partial w}{\partial z} = -\frac{\partial p}{\partial z} + \frac{1}{Re} \nabla^2 w \quad (3)$$

$$\frac{\partial u}{\partial r} + \frac{u}{r} + \frac{1}{r} \frac{\partial v}{\partial \theta} + \frac{\partial w}{\partial z} = 0 \quad (4)$$

where

$$\nabla^2 = \frac{\partial^2}{\partial r^2} + \frac{1}{r} \frac{\partial}{\partial r} + \frac{1}{r^2} \frac{\partial^2}{\partial \theta^2} + \frac{\partial^2}{\partial z^2}$$

where u , v , and w are the perturbation velocities in the radial r , azimuthal θ , and axial z directions, respectively, and p is the perturbation pressure. The preceding equations are nondimensionalized by the mean flow characteristic radius R and the mean axial flow characteristic velocity W_0 . The corresponding Reynolds number is $Re = W_0 R / \nu$, where ν is the kinematic viscosity.

The solutions of Eqs. (1–4) have the form of $\{u, v, w, p\} = \{\hat{u}, \hat{v}, \hat{w}, \hat{p}\} \exp[i(\alpha z + n\theta - \omega t)]$, where \hat{u} , \hat{v} , \hat{w} , and \hat{p} depend on the radius r only. The disturbance is assumed to be periodic in the azimuthal direction, and therefore, the azimuthal wave number n is an integer number. For spatial stability analysis, the axial wave number α is complex and ω is a real frequency (assuming periodic disturbances in time), whereas for the temporal stability analysis α is a real axial wave number (assuming periodic disturbances in the axial direction) and ω is a complex frequency.

Boundary conditions have to be imposed on \hat{u} , \hat{v} and \hat{w} to determine uniquely the solution. The boundary conditions on the centerline ($r = 0$) can be derived using the fact that the velocity vector has a vanishing azimuthal dependence as the centerline is approached. (These conditions were first presented by Batchelor and Gill²⁷ and later were used by Khorrami et al.,²⁸ who applied spectral techniques to calculate eigenmodes in swirling flows.) This requirement yields the following boundary conditions for \hat{u} , \hat{v} , and \hat{w} at $r = 0$:

$$\begin{aligned} \hat{u}, \hat{v} &= 0, & \hat{w} &\text{finite} & \text{for } n &= 0 \\ \hat{u} \pm i\hat{v} &= 0, & 2 \frac{d\hat{u}}{dr} \pm i \frac{d\hat{v}}{dr} &= 0, & \hat{w} &= 0 & \text{for } n = \pm 1 \\ \hat{u}, \hat{v}, \hat{w} &= 0 & \text{for } |n| &> 1 \end{aligned} \quad (5)$$

For confined flows (pipe-type flows) boundary conditions are imposed on the solid wall at $r = 1$ (normalized by the wall radius R). The boundary conditions for a solid wall are given by the no-slip assumption

$$\hat{u}, \hat{v}, \hat{w} = 0 \quad \text{at } r = 1 \quad (6)$$

The boundary conditions (6), together with the boundary conditions on the centerline and the set of equations, constitutes a Sturm–Liouville eigenvalue problem for α (in the spatial case) or ω (in the temporal case). Therefore, in the case of confined flows, there is a complete set of discrete eigenvalues (infinite series of values). The complete solution of the disturbance is the sum of an infinite number of modes associated with these eigenvalues, where the modes coefficients are determined by a given initial condition.

For nonconfined flows (jet-type flows) boundary conditions are required as $r \rightarrow \infty$. When the mean flow velocity components as $r \rightarrow \infty$ are assumed to be

$$\begin{aligned} W &\rightarrow W_\infty, & \frac{dW}{dr} &\rightarrow 0, & V &\rightarrow \frac{\Gamma_\infty}{r} \\ \frac{dV}{dr} &\rightarrow -\frac{\Gamma_\infty}{r^2}, & \text{as } r &\rightarrow \infty \end{aligned} \quad (7)$$

where $W_\infty = W(r \rightarrow \infty)$ and Γ_∞ is the mean flow circulation as $r \rightarrow \infty$, the following asymptotic equation can be deduced:

$$\begin{aligned} \left(\frac{d^2}{dr^2} + \frac{1}{r} \frac{d}{dr} - \frac{1}{r^2} - \mu^2 \right) \left[r^2 \left(\frac{d^2}{dr^2} + \frac{1}{r} \frac{d}{dr} - \frac{1}{r^2} - \alpha^2 \right) \right. \\ \left. \times \left(\frac{d^2}{dr^2} + \frac{1}{r} \frac{d}{dr} - \frac{1}{r^2} - \mu^2 \right) \right] \hat{u} = 0 \end{aligned} \quad (8)$$

where

$$\mu^2 = \alpha^2 + i Re(\alpha W_\infty - \omega)$$

Equation (8) has six independent solutions. As $r \rightarrow \infty$, asymptotic solutions can be found by assuming an asymptotic series of the form

$$\hat{u} = \exp(\lambda r) r^\delta \sum_{k=0}^{\infty} b_k \frac{1}{r^k} \quad (9)$$

This series was originally suggested by Lessen and Paillet⁷ for utilizing a numerical procedure to find discrete modes in the trailing vortex (Batchelor vortex). In the following paragraphs, we use this series to obtain the form of the continuous spectrum in cylindrical columnar flows.

When Eq. (9) is substituted into Eq. (8) and leading terms are compared, the six eigenvalues of λ are found to be $\lambda = \pm \alpha$ and $\lambda = \pm \mu$ (twice). In general, α and μ are complex. In the case where both α and μ have a nonzero real part, three of the six values of λ are physical. In this case, discrete eigenvalues for α or ω can be found. However, if α or μ are pure imaginary ($\alpha = i\sigma$ or $\mu = i\sigma$, where σ is a real number) a continuous spectrum exists:

$$\omega/\alpha = W_\infty - [i(\sigma^2 + \alpha^2)/\alpha Re], \quad 0 \leq \sigma < \infty, \quad Re(\alpha) = 0 \quad (10)$$

Note that the continuous spectrum does not depend on the azimuthal mean velocity of the flow, that is, the continuous spectrum is formed far enough away (theoretically where r tends to infinity), where the mean flow swirl vanishes. In this case, for a given initial condition the complete solution of the disturbance is a superposition of the solution corresponding to the continuous spectrum and the solution corresponding to a finite number of discrete eigenvalues.

Optimal Disturbances

The complete solution for the evolution of a linear disturbance is obtained by solving the initial value problem. In the case of confined flows, where an infinite series of discrete eigenvalues exists, the most unstable mode governs the stability of the flow in long times or distances. In nonconfined flows, the disturbance solution corresponding to the continuous spectrum decays in long times (e.g., see Gustavsson²⁹), and the flow stability, in long times or distances, is again governed by the most unstable discrete mode.

However, in short times or distances, where the decaying modes associated with the initial disturbance are still significant, the solution may yield a substantial transient growth. In confined flows (pipe flows), the large transient growth is due to the nonorthogonal eigenfunctions corresponding to the discrete eigenmodes, whereas in nonconfined flows (jet/wake flows), the continuous spectrum would give rise to the same effect: The continuous spectrum can be approximately discretized by assuming a solid wall at a large radius (theoretically at $r \rightarrow \infty$), where the mean flow is assumed to be uniform.

The maximum disturbance growth can then be found by using the disturbance kinetic energy density

$$E = \int_0^1 (|u|^2 + |v|^2 + |w|^2) r dr \quad (11)$$

for confined flows, where for nonconfined flows the upper bound of the integral is replaced by ∞ . The maximum disturbance amplification is $G = E/E_0$, where E_0 is the disturbance energy density at the initial state. The optimal initial disturbance for which the maximum amplification is attained can be found by the method described by Schmid and Henningson.²³

Results

Stationary Disturbances in Rotating Pipe Flow

The rotating pipe nondimensional base flow is given by

$$U = 0, \quad V = \Omega r, \quad W = 1 - r^2 \quad (12)$$

where the characteristic length R is the pipe radius, the characteristic velocity W_0 is the axial velocity on the centerline, and Ω is the swirl

parameter defined as the ratio between the azimuthal mean velocity on the pipe wall and the axial mean velocity on the centerline.

Unlike Poiseuille pipe flow, rotating pipe flow is characterized by having discrete modes that may grow exponentially. Only a small amount of rotation is required to produce growing discrete modes. Mackrodt³⁰ showed the existence of growing modes for swirl values around $\Omega \approx 3 \times 10^{-4}$ for $Re = 10^5$. Thus, this type of flow is linearly unstable with respect to exponential modes. Nevertheless, in the following paragraphs we attempt to explore the possibility that optimal disturbances, which consist of both growing and decaying modes, may yield a much larger growth in short times or distances.

The eigenvalues and corresponding eigenfunctions of the linear problem are found by using a numerical method formulated in terms of a Chebyshev collocation approximation, following the method of Khorrami et al.²⁸ In this case, 124 polynomials are used. From various tests it is evident that a much smaller number of polynomials is sufficient to obtain accurate eigenvalues. (A detailed discussion regarding the accuracy and precision of the numerical method is given by Khorrami et al.,²⁸ who used about 30–40 polynomials and obtained more than 5-digit accuracy.) However, we chose to increase the number of polynomials up to 124 to obtain smooth eigenfunctions (which Khorrami et al.²⁸ were not concerned about). The optimal disturbances are found by the method used by Reshotko and Tumin²⁴ for Poiseuille pipe flow. The eigenvalue problem and matrix decompositions are carried out using MATLAB[®]. The DM-Suite routines by Weideman and Reddy³¹ are used to obtain the Chebyshev differentiation matrices.

Axissymmetric disturbances ($n=0$), which do not grow exponentially, produce very small amplification factors (less than 3) and, therefore, are not significant from the transient growth mechanism point of view. Azimuthal disturbances ($n=1, 2, \dots$), on the other hand, grow exponentially and may have larger growth rates in short times or distances.

For moderate swirl values, the flow is unstable with respect to convectively evolving disturbances, and therefore, spatial analysis can be applied. Figure 1 shows the complex plane for the axial wave number eigenvalues α for $Re = 3000$, $n=1$, and for a frequency range $\omega = 0-0.8$. (The limits of this range, $\omega=0$ and $\omega=0.8$, for each of the four curves, appear in Fig. 1 next to the endpoints and are marked by the empty and filled-in circles, respectively.) The different lines denote different values of the swirl parameter Ω . Transforming the α plane to the physical one shows that the upper curves correspond to the eigenvalues for which $z > 0$, whereas the lower ones correspond to $z < 0$. For calculations of the transient growth amplification, only the downstream evolving modes, $z > 0$, are to be considered. Furthermore, for the swirl parameter of $\Omega = 0.63$, the upper and lower curves almost coincide, almost creating a pinch point (e.g., see Bers³²). Thus, for values of Ω greater than ~ 0.63 , the flow becomes absolutely unstable.

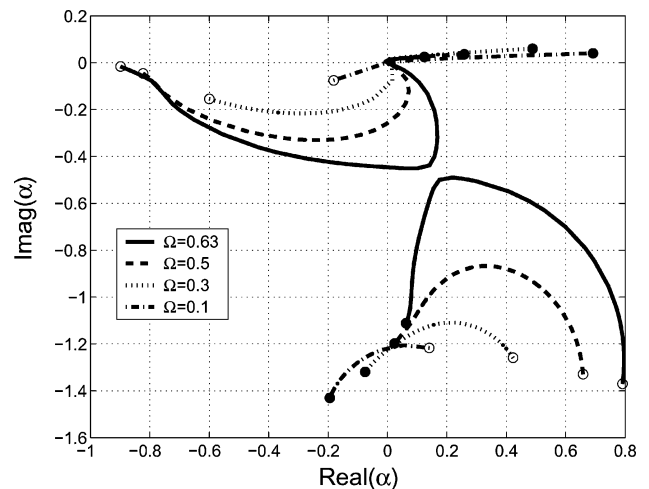


Fig. 1 Discrete modes in the complex axial wavenumber plane for frequency range $\omega = 0-0.8$ and various values of the swirl parameter Ω ; $Re = 3000$ and azimuthal wave number $n = 1$: \circ , $\omega = 0$ and \bullet , $\omega = 0.8$.

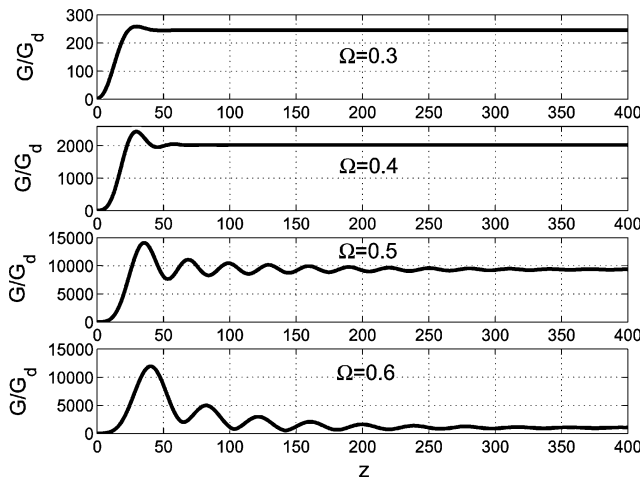


Fig. 2 Amplification ratio A_R vs distance z for four different swirl parameters Ω ; $Re = 3000$, $n = 1$, and $\omega = 0$.

Amplification factors vs distance are found for a Reynolds number $Re = 3000$ and for various azimuthal wave numbers, $n = 1, 2, \dots$, frequencies ω , and swirl parameters Ω . As was stated earlier, exponentially growing modes already exist for small values of Ω . (For $Re = 3000$, growing discrete modes exist for Ω less than 0.05.) Therefore, it is convenient to define the ratio between the optimal amplification factor and the amplification factor of the most unstable discrete mode:

$$A_R(Re, \Omega, n, \omega, \zeta) = \frac{G(Re, \Omega, n, \omega, z = \zeta)}{G_d(Re, \Omega, n, \omega, z = \zeta)} \quad (13)$$

where the discrete amplification factor is

$$G_d(z) = |\exp(i\alpha_d z)|^2$$

and α_d is the eigenvalue that has the largest negative imaginary part for a given set of parameters Re , Ω , n , and ω .

For nonrotating pipe flow, stationary disturbances produce the most significant transient growth, as presented by Reshotko and Tumin,²⁴ and explained analytically by Ben-Dov et al.²⁶ In rotating pipe flow, stationary disturbances can produce substantial growth factors in terms of the ratio A_R . Figure 2 shows the ratio A_R vs the axial distance for four different swirl parameters Ω , where $Re = 3000$ and $n = 1$. It can be seen that a transient effect for A_R exists. In particular, in short distances the optimal disturbance growth rate is greater than the exponential growth of the discrete mode, whereas in long distances A_R is constant, and therefore, the exponential growth rate is the same as that of the discrete mode. Swirl value of $\Omega \sim 0.5$ yields the most significant ratio A_R , where the optimal disturbance yields amplification factors of orders of magnitude larger than the discrete amplification at the same distances.

Figure 3 shows the amplification ratio A_R for three different swirl parameters Ω and three different azimuthal wave numbers n , where $Re = 3000$. Note that the swirl parameter corresponding to the pinch point increases with n . (According to numerical calculations for $n = 2$, the pinch point occurs for $\Omega = 0.83$ and for $n = 3$ it is for $\Omega = 0.98$.) It can be seen that, for small values of Ω , the transient growth is dominated by the higher azimuthal wave numbers. As Ω is increased, effective transient growth is associated with lower azimuthal wave numbers, and beyond a certain threshold of Ω , the azimuthal wave number $n = 1$ is the dominant one.

The results presented in Figs. 2 and 3 imply that in short distances decaying modes may contribute substantially to the growth of linear disturbances. Figure 4 presents the optimal amplification factor normalized by the most unstable mode amplification A_R vs the number of modes involved in the analysis (for stationary spatial modes with $n = 1$ and $\Omega = 0.5$). It can be seen that in this case many decaying modes are required to achieve the order of magnitude of the maximum transient growth. To achieve an accurate convergence, more than 200 decaying modes are involved in the analysis.

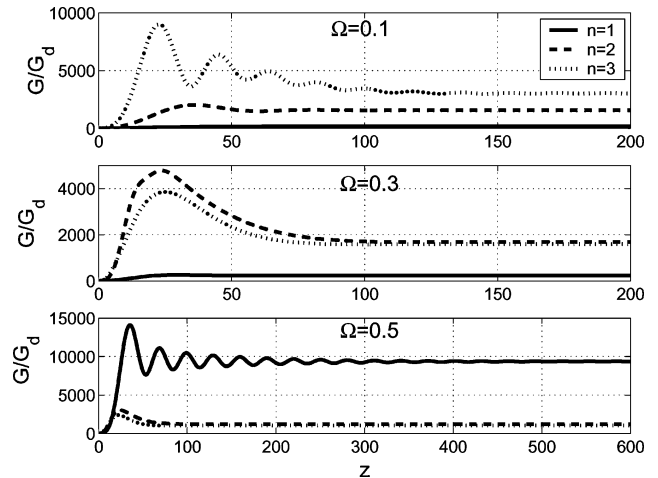


Fig. 3 Amplification ratio A_R vs distance z for three different swirl parameters Ω and three different azimuthal wave numbers n ; $Re = 3000$ and $\omega = 0$.

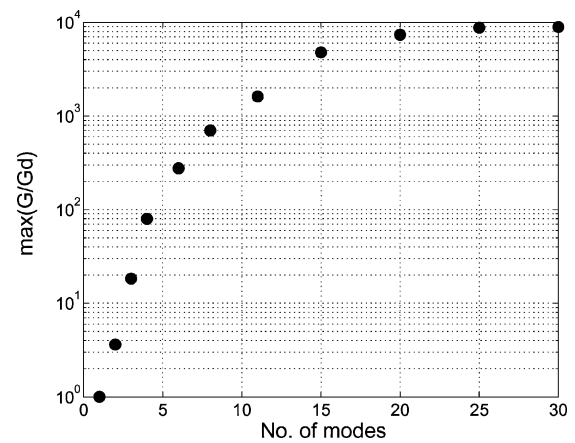


Fig. 4 Maximum amplification ratio curve, $A_{R_{\max}}$ vs number of least stable modes involved in the analysis; $Re = 3000$, $n = 1$, $\omega = 0$, and $\Omega = 0.5$.

In the rotating pipe flow, the optimal disturbance is different in nature from the one in the nonrotating pipe case, which was shown by Ben-Dov et al.²⁶ to be governed by a pair-mode mechanism. They showed that the amplification in the nonrotating pipe case is mostly due to the existence of a pair of least stable modes, having almost the same axial amplitude distribution (with negligible radial and azimuthal components) but opposite phase. The disturbance growth in this case is a result of their cancellation at the initial state. However, in the present case of rotating pipe flow, the initial disturbance is dominated by the most unstable mode, and many decaying modes are required to cancel its amplitude distribution at the initial state. Figures 5a–5c present the velocity distribution of the most unstable mode (dashed curves), the sum of many least stable modes, where the most unstable one is excluded (dotted curves), and the sum of all modes (solid curves), which yield maximum amplification. (For visualization purposes, Figs. 5d–5f show the optimal disturbance distribution in a larger scale.) The initial disturbance in this case corresponds to the parameters $Re = 3000$, $n = 1$, $\omega = 0$, and $\Omega = 0.5$, and it is optimized to yield maximum energy amplification at a distance $z_{\max} = 35$, which is the distance corresponding to the maximum of $A_R = G/G_d$ in Figs. 2 and 3. Evidently, the sum of many decaying modes yields a velocity distribution that is almost parallel to the distribution of the most unstable mode, that is, the most unstable mode has almost the same amplitude distribution but opposite phase compared to the sum of the rest of the modes. Thus, the optimal disturbance energy density is very small at the initial state, and as the disturbance evolves downstream, the most unstable mode becomes dominant, whereas all other modes become negligible.

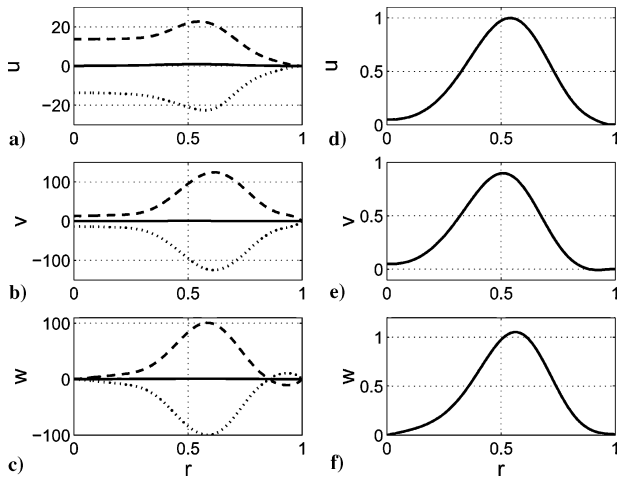


Fig. 5 Rotating pipe flow; $Re = 3000$, $n = 1$, $\omega = 0$, and $\Omega = 0.5$: —, initial velocity distribution of optimal disturbance along pipe radius; ---, most unstable mode only; and, optimal disturbance where most unstable mode is excluded.

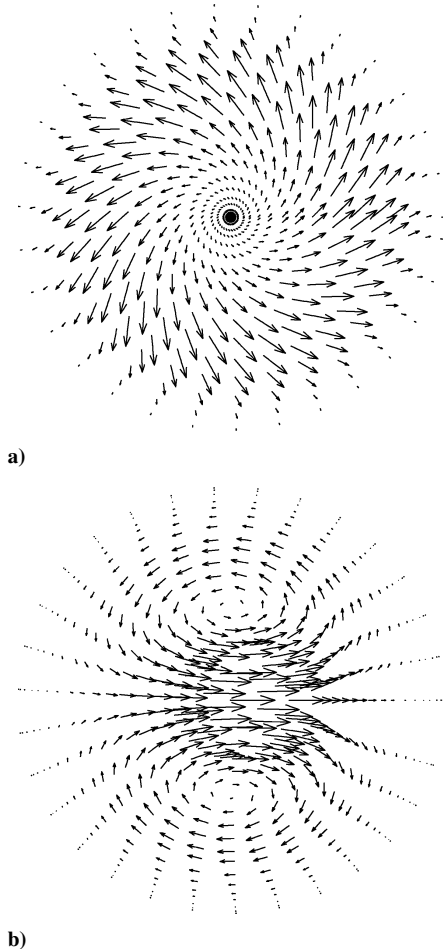


Fig. 6 Initial vector flowfield in the (r, θ) plane for optimal disturbance in rotating and nonrotating pipe flow; $Re = 3000$, $n = 1$, and $\omega = 0$: a) rotating pipe flow with $\Omega = 0.5$ and b) nonrotating pipe flow (from Ben-Dov et al.²⁶).

In Fig. 6 we compare the initial disturbance in the (r, θ) plane for the rotating flow (the same initial disturbance as in Figs. 5a–5f) and the nonrotating flow (from Ben-Dov et al.²⁶). Clearly, the optimal initial disturbance has a different structure in each case: In the nonrotating pipe flow, there is a pair of counter-rotating vortices near the centerline, whereas in the rotating pipe there is a spiral flow with a significant radial velocity component. From Figs. 5a–5f we can also notice that the azimuthal and the axial velocity components

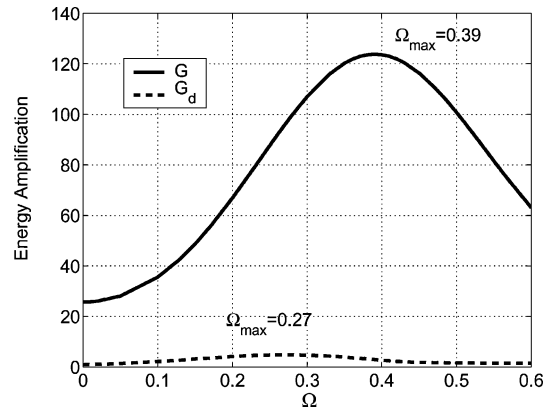


Fig. 7 Optimal amplification and discrete amplification vs swirl parameter Ω in 5 radii distance ($z = 5$) downstream of disturbance initiation position; $Re = 3000$, $n = 1$, and $\omega = 0$.

contribute similarly to the amplification (and even the contribution of the radial component is not negligible), whereas in the nonrotating pipe flow it was shown that at the initial state the axial velocity is dominant.

Figure 7 shows the maximum optimal amplification G and the discrete amplification G_d vs the swirl parameter Ω in a distance z of 5 radii downstream of the disturbance initiation position, where $\omega = 0$, $n = 1$, and $Re = 3000$. Note, again, that in a short distance the optimal amplification may be orders of magnitude larger than the discrete amplification. Furthermore, the swirl value Ω , for which the amplification is the largest, is different from the value corresponding to the maximum amplification of the most amplified discrete mode.

For high values of the swirl parameters Ω (where the flow may be absolutely unstable), it is known that discrete modes become more stable. The optimal disturbances growth in this case is also reduced. In this respect, it is important to mention the work by Pedley,³³ who used asymptotic analysis to examine the linear stability of rapidly rotating pipe flow and found approximate solutions that are Bessel functions. Thus, for high values of Ω , the eigenmodes are approximately a family of orthogonal eigenfunctions and, therefore, can not contribute to the transient effect by an interference mechanism.

Temporal Disturbances in a Trailing Vortex

An important class of three-dimensional longitudinal vortices is the trailing vortex. Batchelor³⁴ presented a similarity solution, which for this type of flow is valid sufficiently far downstream of a wing trailing edge. Following the formulation of Lessen et al.,⁵ the non-dimensional base flow in this case can be written as

$$U = 0, \quad V = (q/r)(1 - e^{-r^2}), \quad W = W_\infty + e^{-r^2} \quad (14)$$

The characteristic radius and velocity are

$$R = \sqrt{4\nu\bar{W}_\infty}$$

$$W_0 = (\bar{\Gamma}_\infty^2/8\nu\bar{z}) \ln(\bar{W}_\infty\bar{z}/\nu) - (L\bar{W}_\infty^2/8\nu\bar{z}) \quad (15)$$

where \bar{W}_∞ and $\bar{\Gamma}_\infty$ are the dimensional velocity and circulation as $r \rightarrow \infty$, respectively, \bar{z} is the dimensional coordinate downstream of the trailing edge, and L is a constant having the dimensions of an area. The swirl parameter q is defined as

$$q = \bar{\Gamma}_\infty/W_0R \quad (16)$$

Lessen et al.⁵ and Leibovich³⁵ argued that translation and inversion of the axial velocity component of the base flow only affects the frequency of the disturbance, whereas the growth rate remains unchanged. (The frequency has a constant shift.) Therefore, it is convenient to choose $W_\infty = 0$ in Eq. (14) for our analysis.

As was shown by Lessen et al.,⁵ in the trailing vortex case exponential growing modes exist for swirl values of $q < 1.5$. The Gaussian profile of the axial flow in Eq. (14) is known to be unstable

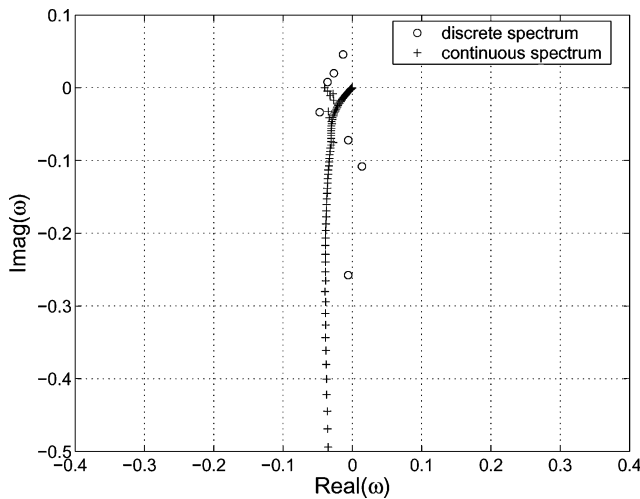


Fig. 8 Eigenvalue spectra in complex frequency plane for the swirl parameter $q=0.2$ and the axial wave number $\alpha=0.2$; $Re=3000$ and $n=-1$.

for modes with azimuthal wave numbers $n = \pm 1$. With the addition of swirl, the modes for which $n < 0$ become highly unstable, with growing rates increasing as $-n$ is increased. In the following paragraphs, we restrict our analysis to the case of $n = -1$, in which the flow is most unstable for moderate values of q .

The numerical procedure in this case was the same as in the preceding subsection. However, in this case, the eigenvalues consist of both discrete and continuous spectra. The temporal eigenvalues were found by using the Chebyshev collocation method as described by Khorrami et al.²⁸ The number of polynomial used in the analysis was 124, and the outer boundary was chosen sufficiently far from the centerline. Results from numerical tests showed that a distance of $120R$ ensures sufficient convergence. (Khorrami et al.²⁸ reported that, for a very moderate number of polynomials, the distance of $100R$ was sufficient and the desired eigenvalues had already converged to four or five significant digits.) Figure 8 presents the least stable modes (for which the growth rate is greater than -0.5) in the complex frequency plane for $Re=3000$, $q=0.2$, and axial wave number $\alpha=0.2$. Notice that exponential growing modes exist in this case (values for which $\text{Im}(\omega) > 0$). Moreover, approximated decaying modes along the imaginary axis, which represent the continuous spectrum in Eq. (10), can be clearly seen. These modes should be along the line $\text{Re}(\omega) = 0$, and the deviation from this line illustrates the accuracy of the continuous spectrum approximation. This result is similar to the result presented by Tumin and Reshotko³⁶ in the case of the continuous spectrum in boundary layers. In both cases, various tests verified that the energy growth is converged within this accuracy of the continuous spectrum.

The optimization method is applied for the complete eigenvalues spectrum (where highly decaying modes are neglected). Amplification factors vs time are found for a Reynolds number $Re=3000$ and azimuthal wave number $n=-1$, in a wide range of axial wave numbers, $\alpha=0-2.5$, for swirl parameters q in the range $0-0.7$.

Figure 9 presents the optimal amplification G and the most unstable exponential mode amplification G_d vs the axial wave number α in a short time of $t=10$ (nondimensionalized by R/W_0), for four different values of the swirl parameter q . It is shown that for low values of q the maximum amplification of the optimal disturbance G takes place for higher values of α compared to the discrete mode amplification G_d . As q is increased from 0 to 0.6, the maxima of the two curves, with respect to α , tend to coincide. Nevertheless, the optimal amplification is shown to be much greater than the exponential amplification. Note that for low values of swirl ($q=0.2$ in Fig. 9) the optimal amplification is much more significant compared to the exponential one (about one order of magnitude difference).

Figure 10 presents the maximum optimal amplification G_{\max} , that is, the maximum of the curves in Fig. 9, and the maximum exponential amplification $G_{d,\max}$ at $t=10$ vs the swirl parameter

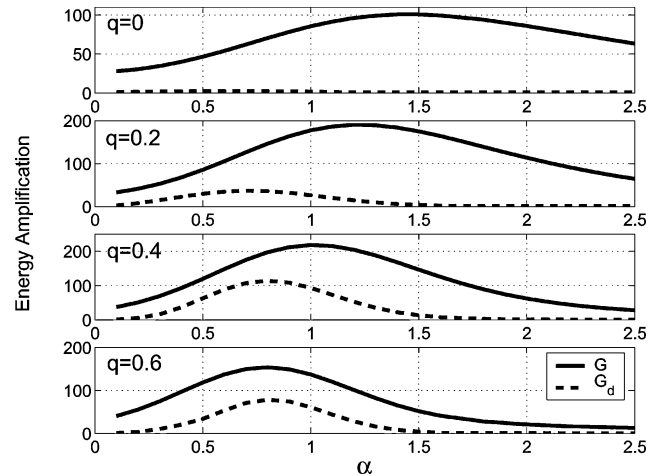


Fig. 9 Optimal amplification and discrete amplification vs axial wave number α at $t=10$, for four different values of the swirl parameter $q=0, 0.2, 0.4$, and 0.6 ; $Re=3000$ and $n=-1$.

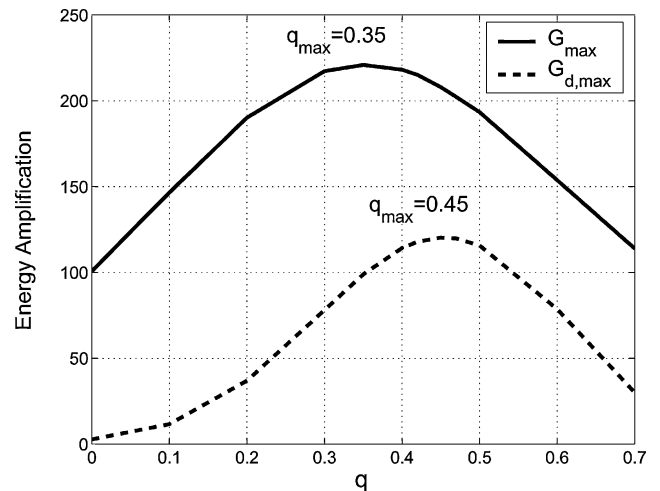


Fig. 10 Maximum optimal amplification and maximum discrete amplification vs swirl parameter q at $t=10$; $Re=3000$ and $n=-1$.

q , where $Re=3000$ and $n=-1$. It can be seen that the optimal amplification is larger than the exponential one. Also note that the swirl value for which the larger optimal amplification is reached is different from the exponential one.

The initial disturbance, which yields the maximum energy amplification, has a similar structure to the optimal initial disturbance in the rotating pipe flow. Figure 11 presents the velocity distribution of the optimal initial disturbance for the parameters $Re=3000$, $n=-1$, $\alpha=1$, and $q=0.35$. This case corresponds to the optimal amplification that is achieved at the time $t=10$. It can be seen that the initial disturbance is concentrated near the centerline in the vicinity of about one radius from the axis. For $r > 1$, the velocity decays rapidly. In Fig. 12, the (r, θ) plane of this initial disturbance is presented for the range $r=0-5$. The disturbance structure seems to have a spiral structure with a significant radial velocity, similar to the structure in the rotating pipe case.

The optimal initial disturbance structure in this case is clearly similar to the one found in the rotating pipe flow. Nevertheless, unlike the rotating pipe flow, in this case the most unstable mode does not play an important role in the optimal growth mechanism; its velocity components are the same order of magnitude as the optimal initial disturbance. In this case, the continuous spectrum contributes mostly to the optimal transient growth. The existence of swirl in the flow does not have a significant effect on the maximum optimal transient growth, whereas the maximum exponential growth is increased significantly when a swirl is added to the flow. In Fig. 9, a

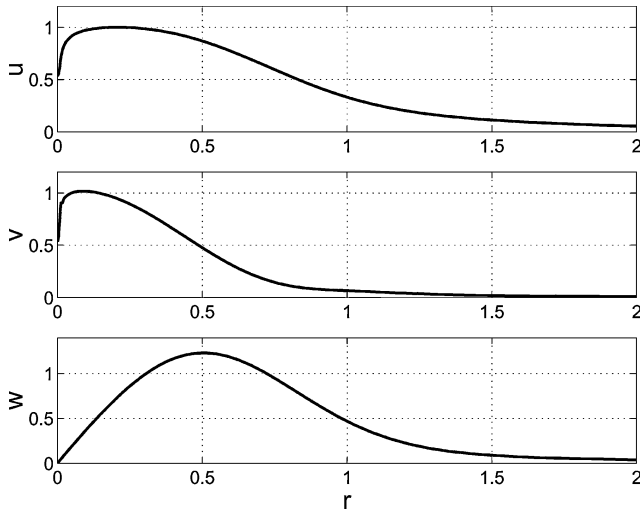


Fig. 11 Initial velocity distribution of trailing vortex optimal disturbance along pipe radius, where maximum amplification is at $t=10$; $Re=3000$, $n=-1$, $\alpha=1$, and $q=0.35$.

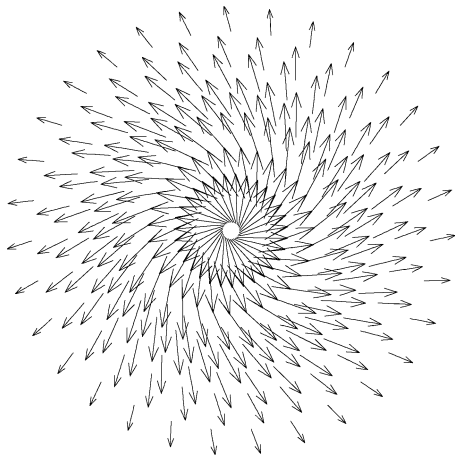


Fig. 12 Initial vector flowfield in (r, θ) plane for optimal disturbance in the trailing vortex for range $r=0-5$, where maximum amplification is at $t=10$; $Re=3000$, $n=-1$, $\alpha=1$, and $q=0.35$.

comparison between the swirling cases, $q=0.2, 0.4$, and 0.6 , and the nonswirling case, $q=0$, demonstrates this argument. This observation is not surprising because, as was pointed out in the preceding section, the continuous spectrum dispersion has no dependence on the mean flow swirl.

Conclusions

The spatial theory of optimal disturbances is applied to rotating pipe flow, in which unstable modes, having exponential growth, exist. It is found that stationary disturbances may yield amplifications of the initial disturbances that are orders of magnitude higher than the amplifications of the most unstable mode only. Furthermore, the maximum growth is achieved by including many decaying modes, in addition to the growing ones. The sum of many decaying modes is needed to cancel the initial velocity distribution of the most unstable mode. Thus, this scenario is different from the mechanism of optimal disturbances in nonrotating pipe flow, where the axial velocity distributions of the pair of least stable modes are canceling each other at the initial state (as explained in detail by Ben-Dov et al.²⁶). The structure of the initial optimal disturbance also has a different nature when the pipe flow is rotated; unlike the structure of two counter-rotating vortices in the pipe flow case, in the rotating pipe case the disturbance flow is spiral with an outward radial component.

The temporal analysis of optimal disturbances is applied to the trailing vortex base flow. In this case, it is found that the continuous

spectrum, which decays over long times, may have an important contribution in short times, when an initial disturbance is assumed. In this case, the optimal initial disturbance has a similar structure to the structure of rotating pipe flow. However, in this case it seems that the transient growth mechanism is not affected significantly by the addition of swirl to the flow.

In both the cases of the rotating pipe and the trailing vortex, it is shown that for a given set of parameters (Reynolds number Re and ω or α) the maximum amplification occurs for different values of the swirl parameter compared to those found for the amplification of normal modes.

Evidently, when the flow is unstable with respect to discrete exponential modes, decaying modes still may make a substantial contribution to the linear stability of the flow in short times or distances, assuming the existence of a particular initial disturbance. Note that a linearly unstable flow, which seems to be governed by an exponential growth mechanism of a single mode only, may be actually governed by a multiple-mode mechanism, when a certain initial disturbance is assumed to exist.

References

- Ash, R. L., and Khorrami, M. R., "Vortex Stability," *Fluid Vortices*, edited by S. I. Green, Kluwer Academic, Norwell, MA, 1995, pp. 317–372.
- Howard, L. N., and Gupta, A. S., "On the Hydrodynamic and Hydro-magnetic Stability of Swirling Flows," *Journal of Fluid Mechanics*, Vol. 14, 1962, pp. 463–476.
- Leibovich, S., and Stewartson, K., "A Sufficient Condition for the Instability of Columnar Vortices," *Journal of Fluid Mechanics*, Vol. 126, 1983, pp. 335–356.
- Barston, E. M., "Circle Theorems for Inviscid Steady Flows," *International Journal of Engineering Science*, Vol. 18, No. 3, 1980, pp. 477–489.
- Lessen, M., Singh, P. J., and Paillet, F., "The Stability of a Trailing Line Vortex. Part 1. Inviscid Theory," *Journal of Fluid Mechanics*, Vol. 63, 1974, pp. 753–763.
- Mayer, E. W., and Powell, K. G., "Viscous and Inviscid Instabilities of a Trailing Vortex," *Journal of Fluid Mechanics*, Vol. 245, 1992, pp. 91–114.
- Lessen, M., and Paillet, F., "The Stability of a Trailing Line Vortex, Part 2, Viscous Theory," *Journal of Fluid Mechanics*, Vol. 65, 1974, pp. 769–779.
- Khorrami, M. R., "On the Viscous Modes of Instability of a Trailing Line Vortex," *Journal of Fluid Mechanics*, Vol. 225, 1991, pp. 197–212.
- Delbende, I., and Chomaz, J. M., and Huerre, P., "Absolute/Convective Instabilities in the Batchelor Vortex: A Numerical Study of the Linear Impulse Response," *Journal of Fluid Mechanics*, Vol. 355, 1998, pp. 229–254.
- Olendraru, C., and Selier, A., and Rossi, M., and Huerre, P., "Inviscid Instability of the Batchelor Vortex: Absolute-Convective Transition and Spatial Branches," *Physics of Fluids*, Vol. 11, No. 7, 1999, pp. 1805–1820.
- Loiseleux, T., and Chomaz, J. M., and Huerre, P., "The Effect of Swirl on Jets and Wakes: Linear Instability of the Rankine Vortex with Axial Flow," *Physics of Fluids*, Vol. 10, No. 5, 1998, pp. 1120–1134.
- Elingsen, T., and Palm, E., "Stability of Linear Flow," *Physics of Fluids*, Vol. 18, No. 4, 1975, pp. 487–488.
- Benney, D. J., and Gustavsson, L. H., "A New Mechanism for Linear and Nonlinear Hydrodynamic Instability," *Studies in Applied Mathematics*, Vol. 64, 1981, pp. 185–209.
- Henningson, D. S., "An Eigenfunction Expansion of Localized Disturbances," *Advances in Turbulence*, Vol. 3, Springer-Verlag, Berlin, 1991, pp. 162–169.
- Reshotko, E., "Transient Growth: A Factor in Bypass Transition," *Physics of Fluids*, Vol. 13, No. 5, 2001, pp. 1067–1075.
- Schmid, P. J., and Henningson, D. S., *Stability and Transition in Shear Flows*, Springer, New York, 2001, pp. 99–151.
- Henningson, D. S., and Gustavsson, L. H., and Breuer, K. S., "Localized Disturbances in Parallel Shear Flows," *Applied Scientific Research*, Vol. 53, 1994, pp. 51–97.
- O'Sullivan, P. L., and Breuer, K. S., "Transient Growth in Circular Pipe Flow. 1. Linear Disturbances," *Physics of Fluids*, Vol. 6, No. 11, 1994, pp. 3643–3651.
- Gustavsson, L. H., "Energy Growth of Three-Dimensional Disturbance in Plane Poiseuille Flow," *Journal of Fluid Mechanics*, Vol. 224, 1991, pp. 241–260.
- Butler, K. M., and Farrell, B. F., "Three-Dimensional Optimal Perturbations in Viscous Shear Flow," *Physics of Fluids A*, Vol. 4, No. 8, 1992, pp. 1637–1650.
- Reddy, S. C., and Henningson, D. S., "Energy Growth in Viscous Channel Flow," *Journal of Fluid Mechanics*, Vol. 252, 1993, pp. 209–238.
- Bergström, L., "Optimal Growth of Small Disturbances in Pipe Poiseuille Flow," *Physics of Fluids A*, Vol. 5, No. 11, 1993, pp. 2710–2720.

²³Schmid, P. J., and Henningson, D. S., "Optimal Energy Density Growth in Hagen-Poiseuille Flow," *Journal of Fluid Mechanics*, Vol. 277, 1994, pp. 197-225.

²⁴Reshotko, E., and Tumin, A., "Spatial Theory of Optimal Disturbances in a Circular Pipe Flow," *Physics of Fluids*, Vol. 13, No. 4, 2001, pp. 991-996.

²⁵Ashpis, D. E., and Reshotko, E., "The Vibrating Ribbon Problem Revisited," *Journal of Fluid Mechanics*, Vol. 213, 1990, pp. 531-547.

²⁶Ben-Dov, G., Levinski, V., and Cohen, J., "On the Mechanism of Optimal Disturbances: The Role of a Pair of Nearly Parallel Modes," *Physics of Fluids*, Vol. 15, No. 7, 2003, pp. 1961-1972.

²⁷Batchelor, G. K., and Gill, A. E., "Analysis of the Stability of Axisymmetric Jets," *Journal of Fluid Mechanics*, Vol. 14, 1962, pp. 529-551.

²⁸Khorrami, M. R., and Malik, M. R., and Ash, R. L., "Application of Spectral Collocation Techniques to the Stability of Swirling Flows," *Journal of Computational Physics*, Vol. 81, No. 1, 1989, pp. 206-229.

²⁹Gustavsson, L. H., "Initial-Value Problem for Boundary Layer Flows," *Physics of Fluids*, Vol. 22, No. 9, 1979, pp. 1602-1605.

³⁰Mackrodt, P. A., "Stability of Hagen-Poiseuille Flow with Super-

imposed Rigid Rotation," *Journal of Fluid Mechanics*, Vol. 73, 1976, pp. 153-164.

³¹Weideman, J. A. C., and Reddy, S. C., "A MATLAB Differentiation Matrix Suite" [available online], URL: <http://dip.sun.ac.za/~weideman/research/differ.html> [cited 29 Aug. 2003].

³²Bers, A., "Space-Time Evolution of Plasma Instabilities—Absolute and Convective," *Handbook of Plasma Physics*, edited by A. A. Galeev and R. N. Sudan, Vol. 1, North-Holland, Amsterdam, 1983, Chap. 3.2, pp. 452-516.

³³Pedley, T. J., "On the Instability of Viscous Flow in a Rapidly Rotating Pipe," *Journal of Fluid Mechanics*, Vol. 35, 1969, pp. 97-115.

³⁴Batchelor, G. K., "Axial Flow in Trailing Line Vortices," *Journal of Fluid Mechanics*, Vol. 20, 1964, pp. 645-658.

³⁵Leibovich, S., "Vortex Stability and Breakdown: Survey and Extension," *AIAA Journal*, Vol. 22, 1984, pp. 1192-1206.

³⁶Tumin, A., and Reshotko, E., "Spatial Theory of Optimal Disturbances in Boundary Layers," *Physics of Fluids*, Vol. 13, No. 7, 2001, pp. 2097-2104.

J. Gore
Associate Editor

Elements of Spacecraft Design

Charles D. Brown, *Wren Software, Inc.*

This new book is drawn from the author's years of experience in spacecraft design culminating in his leadership of the Magellan Venus orbiter spacecraft design from concept through launch. The book also benefits from his years of teaching spacecraft design at University of Colorado at Boulder and as a popular home study short course.

The book presents a broad view of the complete spacecraft. The objective is to explain the thought and analysis that go into the creation of a spacecraft with a simplicity and with enough worked examples so that the reader can be self taught if necessary. After studying the book, readers should be able to design a spacecraft, to the phase A level, by themselves.

Everyone who works in or around the spacecraft industry should know this much about the entire machine.

Table of Contents:

- | | | |
|----------------------|---------------------------|--|
| ❖ Introduction | ❖ Power System | ❖ Appendix A: Acronyms and Abbreviations |
| ❖ System Engineering | ❖ Thermal Control | ❖ Appendix B: Reference Data |
| ❖ Orbital Mechanics | ❖ Command And Data System | ❖ Index |
| ❖ Propulsion | ❖ Telecommunication | |
| ❖ Attitude Control | ❖ Structures | |

AIAA Education Series

2002, 610 pages, Hardback • ISBN: 1-56347-524-3 • List Price: \$111.95 • **AIAA Member Price: \$74.95**

American Institute of Aeronautics and Astronautics
Publications Customer Service, P.O. Box 960, Herndon, VA 20172-0960
Fax: 703/661-1501 • Phone: 800/682-2422 • E-mail: warehouse@aiaa.org
Order 24 hours a day at www.aiaa.org



American Institute of Aeronautics and Astronautics

02-0547

